JOURNAL OF SPACECRAFT AND ROCKETS
Vol. 46, No. 1, January–February 2009

Uncertainty Analysis of a Large-Scale Satellite Finite Element Model

Gerhart I. Schuëller*
University of Innsbruck, 6020 Innsbruck, Austria
Adriano Calvi†
ESA, 2200 AG Noordwijk, The Netherlands
Manuel F. Pellissetti‡ and Helmut J. Pradlwarter§
University of Innsbruck, 6020 Innsbruck, Austria
Sebastiaan H. J. A. Fransen¶
ESA, 2200 AG Noordwijk, The Netherlands
and
Andreas Kreis**
Andreas Kreis Consultancies, 7212 Seewis-Dorf, Switzerland

DOI: 10.2514/1.32205

The effects of uncertainties in the material properties and the geometry of a satellite structure are investigated for various aspects of the structural performance. The underlying numerical model is a refined large-scale finite element model, which naturally implies a large number of uncertain parameters. To cope with the computational challenge associated with the large number of parameters, recently developed advanced Monte Carlo simulation methods are applied. Because of their insensitivity with respect to the number of uncertain parameters, these methods are suitable for large-scale finite element models arising in aerospace applications. The numerical results indicate significant scatter in the quantities of interest and hence emphasize the importance of accounting for uncertainties in the numerical model to rationally assess the structural performance and to ensure its reliability. Furthermore, the paper demonstrates that due to the efficiency of the adopted uncertainty analysis methods, the associated computational efforts are greatly reduced and hence manageable, if compared with traditional methods.

Nomenclature

$\mathbf{C}$	=	damping matrix
COV	=	coefficient of variation (σ/μ)
d	=	dimension of vector $\mathbf{X}$ (number of uncertain input parameters)
F	=	failure set
$\mathbf{F}$	=	force vector
F_{sliding}	=	sliding force at the solar-panel connector beam
$F_{\mathbf{X}}(\mathbf{x})$	=	joint cumulative distribution function of $\mathbf{X}$
f	=	excitation frequency in frequency response analysis
$g(\mathbf{X})$	=	performance function indicating the state of a structure
$\mathbf{K}$	=	stiffness matrix
$\mathbf{M}$	=	mass matrix
$M_{n,m}$	=	set of matrices with n rows and m columns
m	=	number of modes retained in modal expansion
N	=	number of samples
N_p	=	sample number of p percentile in set $\{\hat{R}^{(k)}\}_{k=1}^{N}$
n	=	number of degrees of freedom of the finite element model
$P[\cdot]$	=	probability
p_F	=	probability of failure
$\hat{p}_F$	=	estimate of the probability of failure
$\mathbf{R}$	=	vector of the response quantities of interest
$\{\hat{R}^{(k)}\}_{k=1}^{N}$	=	elements of set $\{R^{(k)}\}_{k=1}^{N}$ sorted in increasing order
$\mathcal{S}$	=	sample space
S	=	safe set
s_j	=	response sensitivity with respect to x_j
$\tilde{s}_j$	=	partial derivative with respect to x_j
t	=	time
$\bar{\mathbf{u}}$	=	complex displacement vector
var	=	variance
$\mathbf{X}$	=	vector or uncertain input parameters of the model
X_j	=	jth uncertain parameter
$\mathbf{X}^{(k)}$	=	kth sample of vector $\mathbf{X}$
x_j	=	deterministic variable corresponding to X_j
$\bar{\mathbf{z}}$	=	vector of modal coordinates
$\bar{z}_j$	=	modal coordinates
Δx_j	=	finite (small) perturbation of parameter x_j
δ_{rs}	=	Kronecker delta
ζ_j	=	modal damping ratio of the jth mode
θ	=	random event
λ_j	=	original (unmodified) jth eigenvalue
μ	=	mean
$\hat{\lambda}_i$	=	representation of the ith eigenvalue by weighted superposition
σ	=	standard deviation
$\sigma_{\hat{p}_F}$	=	standard deviation of the failure probability estimate
$\mathbf{\Phi}$	=	matrix of normal modes
$\mathbf{\Phi}^{(k)}$	=	matrix of normal modes of the kth sample
ϕ_j	=	jth normal mode

Received 17 May 2007; revision received 9 May 2008; accepted for publication 25 July 2008.

*Professor and Chair, Institute of Engineering Mechanics, Technikerstrasse 13; Mechanik@uibk.ac.at.

†Project Manager, Structures Section, European Space Research and Technology Centre, P.O. Box 299; adriano.calvi@esa.int. Professional Member AIAA.

‡Postdoctoral Fellow, Institute of Engineering Mechanics.

§Associate Professor, Institute of Engineering Mechanics.

¶Consultant, Structures Section, Advanced Operations and Engineering Services Group B.V.; bas.fransen@aoes.com. Professional Member AIAA.

**Consultant, Crestacalva 150, 7212 Seewis-Dorf; andreas.kreis@akrs.ch. Professional Member AIAA.

$\boldsymbol{\Psi}$ = matrix of weights
ψ_{ij} = weight of the jth eigenvalue with respect to the ith eigenvector
ω_j = jth eigenfrequency
$1_F(\mathbf{X})$ = indicator function of the failure set

Subscript

MC = Monte Carlo simulation

Superscripts

(k) = kth sample
(0) = nominal sample (all input parameters assume their mean value)

I. Introduction

THE importance of rationally treating uncertainties in numerical models of structures is widely recognized, not only in the aerospace community, but also in other fields of engineering faced with the task of ensuring the reliability of structural performance. In their daily work, aerospace structural engineers deal with the unavoidable uncertainties by resorting to safety factors [1,2]. Although in most cases this approach undoubtedly alleviates a great portion of the detrimental effects of uncertainties on the usefulness of numerical models as predictive tools, it cannot be regarded as a truly rational basis for quantifying and managing uncertainties in predictive models.

In contrast, the application of probabilistic reasoning to those aspects of the model that are affected by uncertainties does allow the rational treatment and propagation of uncertainties and hence the assessment of their effect on the structural performance. More specifically, in the probabilistic approach to uncertainty quantification, those parameters of the numerical model that are associated with uncertainty are modeled as random variables. The distribution type and the distribution parameters of the random variables are typically based on experimental data or other pieces of information, as well as on the experience of the analyst. In the absence of solid evidence suggesting otherwise, normal, log normal, or uniform distributions are frequently assumed for convenience.

Clearly, any assumption for the distribution of the model parameters associated with uncertainties, which deviates significantly from the actual distribution, may negatively affect the accuracy of the results of the uncertainty analysis. Consequently, the probability distribution of the uncertain parameters is to be specified with care (and if necessary additional data should be collected), in particular for parameters that have a strong impact on the response quantities of interest.

In this context, it should be noted that uncertainty quantification of computational models has been identified by the Performance Test Committee 60 of the American Society of Mechanical Engineers (ASME) [3] as an integral part of the validation process with which the credibility of numerical solid mechanics models can be improved. The preceding ASME document attaches additional weight to uncertainty quantification of numerical models, as it states that validation should only be performed with a computational model in which uncertainties are quantified.

A significant obstacle to the application of probabilistic analysis methods to numerical models of complex structures, such as satellite structures, is posed by the associated computational efforts. As the finite element models become more refined, the number of model parameters affected by uncertainty grows significantly. Unfortunately, for many probabilistic analysis methods, the associated computational effort grows even exponentially with the number of uncertain parameters, quickly reaching prohibitive levels.

A possible solution to this problem is then to reduce, based on engineering judgment, the number of uncertain parameters by treating those parameters with a modest influence on the response as deterministic. The problem with this approach is that the more complex a structure, the more difficult it is (even for a most experienced engineer) to separate important parameters from unimportant ones.

The approach pursued in this paper, ultimately aiming at the efficient uncertainty and reliability analysis of a large-scale finite element (FE) model of a satellite structure with a large number of uncertain parameters, is mainly based on Monte Carlo simulation. Simulation-based methods are generally known to be less sensitive to the number of uncertain parameters than approximate methods and are therefore more suitable for the analysis of large-scale problems. This has long been known for the *direct Monte Carlo* simulation method: its accuracy is, in fact, independent of the number of input random variables and only depends on the number of samples used to synthesize the estimator for the quantity of interest (see, for example, [4]). More specifically, the accuracy is proportional to $\sqrt{N}$, where N is the number of samples. In the present paper, direct Monte Carlo simulation is used to assess the uncertainty in the eigenfrequencies and in selected quantities of interest, in terms of the probability distribution functions and of the fractiles.

The main problem of direct Monte Carlo simulation is related to computational efficiency in the context of highly reliable structures. In this case, the event of interest (namely, failure) is extremely rare and the accuracy is then significantly deteriorated, because it is proportional to $\sqrt{p_F}$, where p_F is the probability of failure.

In the context of satellite structural design, the reliability requirements are naturally very high. In view of the preceding, the reliability analysis of a satellite with direct Monte Carlo is prohibitively expensive, even if the underlying numerical (FE) model is only moderately complex. On the other hand, performing the reliability analysis with a highly simplified and hence less computationally intensive model would defy the purpose, because the quantitative results of a probabilistic analysis will be, at best, as good as the numerical model used in the process.

Improved versions of Monte Carlo simulation, often referred to as variance-reduction techniques, have been developed with the objective to increase the accuracy for a given number of samples. With particular consideration for the problems of structural reliability analysis, several powerful methods have recently been proposed, such as subset simulation [5] and line sampling [6]. In the present paper, these methods are instrumental for assessing the reliability of a satellite structure, considering that extremely high levels of reliability are of interest (i.e., the failure probability is only about 1 in a million).

Monte Carlo simulation can also be successfully employed in the context of a different issue of great relevance for uncertainty analysis: namely, the classification of the sources of uncertainty with respect to their importance on a given quantity of interest. A method for performing such a stochastic sensitivity analysis with moderate computational efforts has recently been proposed [7,8]. The present paper reports the results of this method for the considered satellite structure by indicating those uncertain parameters that account for the largest part of the uncertainty in the quantity of interest that therefore most affect the reliability of the structure. This information is particularly valuable for experimental testing campaigns, as it indicates which parameters should be characterized most accurately to reduce the uncertainty in the quantities of interest.

II. Methods of Analysis

A. Deterministic Mechanical Model

1. General Remarks

In this section, the deterministic mechanical and mathematical models, which are underlying the probabilistic analysis, are briefly reviewed. In view of the applications dealt with in the present paper, emphasis lies on dynamic analysis methods for aerospace structures. More specifically, the mode displacement method for analyzing the dynamic structural response is summarized. More detailed aspects of the methods may be found in the pertinent literature [9,10].

2. Frequency Response Analysis: Mode Displacement Method

The equation of motion of a viscoelastic structure, discretized with finite elements, under harmonic excitation is (see, for example, [9])

$$\mathbf{M}\,\ddot{\bar{\mathbf{u}}}(t) + \mathbf{C}\dot{\bar{\mathbf{u}}}(t) + \mathbf{K}\bar{\mathbf{u}}(t) = \mathbf{F}e^{i\Omega t} \tag{1}$$

where $\mathbf{M}$, $\mathbf{C}$, and $\mathbf{K}$ denote the mass, damping, and stiffness matrices, respectively, and $\bar{\mathbf{u}}$ is the complex displacement vector, for which the real component is the actual steady-state response.

In the mode displacement method, the response $\bar{\mathbf{u}}$ is expressed as

$$\bar{\mathbf{u}}(t) = \sum_{j=1}^{N} \phi_j \bar{z}_j(t) = \mathbf{\Phi}\bar{\mathbf{z}}(t), \qquad \bar{\mathbf{u}}(t) \approx \sum_{j=1}^{m} \phi_j \bar{z}_j \tag{2}$$

The set of normal modes $\{\phi_j\}_{j=1}^{N}$ results from the solution of the generalized eigenvalue problem:

$$\left(-\omega_j^2\mathbf{M} + \mathbf{K}\right)\phi_j = 0 \tag{3}$$

Furthermore, the coefficients $\bar{z}_j$ are given as follows:

$$\bar{z}_j = \frac{\mathbf{\Phi}^t\mathbf{F}}{-\Omega^2 + 2i\Omega\zeta_j\omega_j + \omega_j^2} \tag{4}$$

where ζ_j are the modal damping ratios.

The second part of Eq. (2) represents the truncation after the m lowest eigenfrequencies, which is commonly applied to systems with a large number of degrees of freedom (DOF). Once the displacements $\bar{\mathbf{u}}(t)$ have been computed, other quantities of interest such as stresses, internal forces, and accelerations can be recovered using so-called output transformation matrices.

B. Uncertainty Quantification: Concept and Tools

1. General Remarks

The deterministic analysis methods described in the previous section constitute efficient predictive tools in the design and verification process. In fact, no designer or analyst will perceive these predictions as purely deterministic because of the significant uncertainties arising in the finite element modeling process, in particular, with respect to the parameters of the model.

With the help of probabilistic methods, this intuitive awareness of the unavoidable uncertainties is superseded by a rational quantitative framework within which uncertainties are processed and controlled. The uncertain quantities of the numerical model are collected in a random vector:

$$\mathbf{X} = [X_1 \quad X_2 \quad \cdots \quad X_d\,], \qquad X_i = X_i(\theta), \qquad \theta \in \mathcal{S} \tag{5}$$

where θ denotes the random event, $\mathcal{S}$ is the sample space, and d is the dimension of the random vector $\mathbf{X}$. The latter is fully characterized by its joint cumulative distribution function (CDF):

$$F_{\mathbf{X}}(\mathbf{x}) = P[X_1 \le x_1, X_2 \le x_2, \ldots, X_d \le x_d] \tag{6}$$

where $\mathbf{x} = [x_1\ x_2\ \cdots\ x_d]$ are deterministic, and $P[\cdot]$ denotes the probability. The randomness in the parameters propagates to the system matrices [e.g., in Eq. (1)] and hence to the response

$$\begin{gathered} \mathbf{M} = \mathbf{M}(\theta), \qquad \mathbf{C} = \mathbf{C}(\theta), \qquad \mathbf{K} = \mathbf{K}(\theta) \\ \mathbf{F} = \mathbf{F}(\theta) \qquad \longrightarrow \qquad \mathbf{u} = \mathbf{u}(\theta) \end{gathered} \tag{7}$$

The objective of the uncertainty analysis is to estimate the CDF $F_{\mathbf{R}}(\mathbf{r})$ of the response quantities of interest $\mathbf{R} = \mathbf{R}(\mathbf{u}(\theta))$.

To ensure the applicability of probabilistic methods to the analysis of industrial applications, such as the satellite considered in this paper, it is of paramount importance that these methods be *scalable*. This means that the performance must not deteriorate catastrophically when the size of the FE model increases. Many methods do suffer this fate, because they are sensitive to the dimension of the random vector $\mathbf{X}$, and (quite naturally) the dimension of $\mathbf{X}$ is usually proportional to the size of the FE model. The procedures described in the sequel are simulation-based and exhibit the desired scalability in most cases. This characteristic has been confirmed in the probabilistic treatment of a set of large FE analysis tasks described in Sec. III.

2. Monte Carlo Simulation

It is well known that for the task of estimating the response CDF $F_{\mathbf{R}}(\mathbf{r})$, the direct Monte Carlo simulation (MCS) method is robust (see, for example, [11]); however, this procedure is very inefficient when statements about low-probability events are sought. In the direct MCS, samples of the input random vector $\mathbf{X}$ are generated, such that the ensemble $\{\mathbf{X}^{(k)}\}_{k=1}^{N}$ matches the required CDF of the input vector, $F_{\mathbf{X}}(\mathbf{x})$, in Eq. (6). For each sample $\mathbf{X}^{(k)}$ of the input vector, the corresponding sample response $R^{(k)}$ is evaluated, and from the ensemble, the desired response CDF can be estimated, typically in the form of fractiles R_p, which indicate the response level associated with a given probability level p. These can be approximated as follows:

Let $\{R^{(k)}\}_{k=1}^{N}$ be the ensemble of responses obtained by performing N MCS runs and let $\{\hat{R}^{(k)}\}_{k=1}^{N}$ contain the elements of $\{R^{(k)}\}$, but in increasing order:

$$\{\hat{R}^{(k)}\}_{k=1}^{N}, \qquad \hat{R}^{(1)} \le \hat{R}^{(2)} \le \cdots \le \hat{R}^{(N)} \tag{8}$$

Then

$$R_p \approx \hat{R}^{(N_p)}, \qquad N_p = \text{round}\,[p \cdot N], \qquad 1 \le N_p \le N \tag{9}$$

where the operator round $[\cdot]$ rounds the argument to the nearest integer. The corresponding confidence interval for the fractile R_p is given as follows (see, for example, [12]):

$$\hat{R}^{(N_p - m)} < R_p < \hat{R}^{(N_p + m)} \tag{10}$$

where

$$m \approx \Phi^{-1}\left(\frac{\gamma}{2} + \frac{1}{2}\right)\sqrt{Np(1-p)}$$

where Φ^{-1} is the inverse cumulative distribution function of the standard normal random variable and γ is the confidence level.

3. Assessment of Modal Scatter

The eigenfrequencies resulting from Eq. (3) are among the key parameters for the dynamic behavior of spacecraft structures. They play a central role, for example, in the context of mechanical testing [13] and of finite element model updating [14]; consequently, the associated uncertainty is of great interest.

To capture the scatter correctly it is indispensable to avoid intermixing of eigenfrequencies from one simulation to the next, which correspond to modes that are physically unrelated. In the present study this is accomplished by expressing the eigenvalues of each simulation as a weighted superposition:

$$\hat{\lambda}_i^{(k)} = \sum_j \lambda_j^{(k)} \left[\psi_{ij}^{(k)}\right]^2 \tag{11}$$

where $\hat{\lambda}_i^{(k)}$ denotes the modified eigenvalue associated with the ith eigenmode and $\{\lambda_j^{(k)}\}$ is the set of sample eigenvalues. The weights $\{\psi_{ij}\}$ are given by the following expression:

$$\mathbf{\Psi}^{(k)} = \mathbf{\Phi}^{(0)^T}\mathbf{M}^{(0)}\mathbf{\Phi}^{(k)}, \qquad \mathbf{\Psi}^{(k)^T}\mathbf{\Psi}^{(k)} = \mathbf{I} \tag{12}$$

where the superscript 0 indicates the nominal case. The physical meaning of the matrix $\mathbf{\Psi}^{(k)}$ can be visualized by considering that

$$\mathbf{\Phi}^{(k)} = \mathbf{\Phi}^{(0)}\mathbf{\Psi}^{(k)}, \qquad \mathbf{\Phi}^{(k)}, \qquad \mathbf{\Phi}^{(0)} \in M_{n,m}, \qquad \mathbf{\Psi}^{(k)} \in M_{m,m} \tag{13}$$

where n is the number of DOF of the FE model and m is the dimension of the modal basis (i.e., the number of modes that are retained). Hence, the matrix $\mathbf{\Psi}^{(k)}$ transforms the nominal eigenvectors $\mathbf{\Phi}^{(0)}$ to the eigenvectors of the sample k.

4. Sensitivity Analysis: Gradient Estimation

The sensitivity of response quantities of interest to the variability of input parameters is of importance, irrespective of whether a deterministic or probabilistic approach is taken. In general, the sensitivities provide improved understanding of the mechanical and numerical models, for example, in the context of model updating and model validation. This way, excessive, possibly pathological, sensitivities can be detected and eliminated.

The most widely used sensitivity measure is the set of partial derivatives of a response quantity of interest r with respect to the input parameters under consideration:

$$\tilde{s}_j = \left.\frac{\partial r}{\partial x_j}\right|_{\mathbf{x}=\mathbf{x}^{(0)}} \tag{14}$$

where $\mathbf{x}^{(0)}$ is the nominal value (e.g., the mean) of the vector collecting the input parameters. If the input parameters $\{x_j\}_{j=1}^{d}$ are affected by uncertainty, a more meaningful sensitivity measure for the response is one that accounts for the magnitude of the variations of these parameters, such as

$$s_j = \left.\frac{\partial r}{\partial x_j}\right|_{\mathbf{x}=\mathbf{x}^{(0)}} \sigma_{x_j} \tag{15}$$

In this case, the partial derivative is postmultiplied by the standard deviation σ_{x_j} of the corresponding input parameters. This yields dimensionally homogeneous sensitivity measures, thus allowing a direct comparison of the relative importance of the individual parameters.

Most FE codes do not analytically compute the partial derivatives of responses with respect to the input parameters, formulated in Eq. (14). It is then possible to approximate the derivatives using finite differences:

$$\tilde{s}_j = \frac{\partial r}{\partial x_j} \approx \frac{r(\bar{\mathbf{x}} + [0 \cdots 0 \Delta x_j 0 \cdots 0]^T) - r(\bar{\mathbf{x}})}{\Delta x_j} \tag{16}$$

where Δx_j is sufficiently small for the response to remain within the quasi-linear range and sufficiently large to retain enough significant digits. Although a full finite-difference-based sensitivity analysis (i.e., the evaluation of the partial derivatives with respect to all input parameters under consideration) is usually feasible for a moderate number d of input parameters, for large complex FE models with many input parameters affected by uncertainty, the approach becomes quickly prohibitive.

This problem is often circumvented by postulating a small set of the most important input parameters. However, for complex systems, such an assumption is questionable, because important parameters might not be easily identifiable and therefore would be missed.

Recently, a novel gradient estimation tool has been developed [7] that remains highly efficient even for very large values of d. The total number of FE analyses, however, depends on the number of parameters that have a strong impact on the response and only to a small extent on the dimension d. The algorithm exploits the fact that for most problems, the scatter in a particular response quantity is mainly influenced by a more or less small subset of the uncertain parameters. In these cases, the algorithm will be able to identify, by requiring rather few samples, the influential input parameters. A most significant gain in the computational efficiency is then achieved by computing the partial derivatives, according to Eq. (16), *only* for the most influential input parameters.

The key idea of the algorithm consists of generating Monte Carlo samples of the input parameters in the neighborhood of that point of the input parameter space for which the gradient is sought. The corresponding output quantities of interest are computed for these samples, and the correlation coefficients between the input parameters and the output quantities of interest are computed. An importance ranking of the input parameters is then performed based on the correlations, and the sensitivity with respect to the most important parameters is computed using a finite difference approximation. The algorithm proceeds iteratively until the desired accuracy is achieved. A more detailed description of the algorithm is included in Appendix A; for more detail, the reader is referred to [7].

The remarkable efficiency of this novel algorithm is demonstrated for large-scale applications in [8]: for a refined FE model with roughly 1300 uncertain input parameters, the most influential parameters are identified using merely 150 samples (i.e., $\approx$11% of the FE runs needed for a sensitivity analysis involving all uncertain parameters). In another example, less than 800 samples are needed to identify the most influential parameters from a total of 34,000 parameters; the cost is only about 2.5% of that required by a full sensitivity analysis.

In the present paper, the efficiency of the algorithm is essential for identifying the most influential uncertain parameters of the considered satellite FE model (cf. Sec. III.C.4).

5. Estimation of Small Failure Probabilities

a. Structural Reliability. The assessment of the reliability of structures requires a quantitative definition of failure. For this purpose, it is common practice to define a so-called performance function $g(\mathbf{X})$, which characterizes the state of the structure and which is therefore a function of the vector of the uncertain parameters $\mathbf{X}$:

$$g(\mathbf{X}) \quad \text{such that} \begin{cases} g(\mathbf{X}) > 0 \Longleftrightarrow \mathbf{X} \in S \\ g(\mathbf{X}) < 0 \Longleftrightarrow \mathbf{X} \in F \\ g(\mathbf{X}) = 0 \Longleftrightarrow \text{limit state} \end{cases} \tag{17}$$

where S and F denote the safe set and the failure set, respectively. The reliability of a structure can then be quantified by its complementary quantity, the probability of failure p_F:

$$p_F = P[\mathbf{X} \in F] = \int_F f_{\mathbf{X}}(\mathbf{x}) \mathrm{d}\mathbf{x} = \int 1_F(\mathbf{x}) f_{\mathbf{X}}(\mathbf{x}) \mathrm{d}\mathbf{x} \tag{18}$$

where

$$1_F(\mathbf{X}) = \begin{cases} 0 \Longleftrightarrow \mathbf{X} \in S \\ 1 \Longleftrightarrow \mathbf{X} \in F \end{cases}$$

which is denoted as the indicator function. Although conceptually simple, the evaluation of the preceding integral is usually a complex task, particularly when applied to large-scale structural systems, mainly because the evaluation of the indicator function is usually time-consuming. Numerous methods for its estimation have been devised in the past; in the present paper, a recently proposed novel method denoted as line sampling is advocated for the analysis of large-scale structures. The method exploits information about the structural model to reduce the required number of samples and hence the CPU time. For this reason, it belongs to the class of the so-called variance-reduction methods [15].

b. Monte Carlo Simulation and Variance-Reduction Methods. The direct MCS estimator for the probability of failure $p_F = P[F]$, where F denotes the failure event, has the form

$$\hat{p}_{F,\mathrm{MC}} = \frac{1}{N} \sum_{k=1}^{N} 1_F(\mathbf{X}^{(k)}) \tag{19}$$

In the preceding equation, N is the number of samples, $\mathbf{X}^{(k)}$ denotes the kth realization of the set of input variables, and $1_F(\mathbf{X}^{(k)})$ is the indicator function of the failure event, which takes the value of 1 if $\mathbf{X}^{(k)}$ leads to failure and takes 0 otherwise. It should be noted that the evaluation of the indicator function is the computationally most expensive part, because it is usually necessary to perform a full FE analysis to determine whether the combination of input parameters $\mathbf{X}^{(k)}$ leads to failure. The variance of this estimator, expressed by the

coefficient of variation (COV)

$$\mathrm{COV}_{\mathrm{MC}} = \frac{\sqrt{\mathrm{var}[\hat{p}_F]}}{p_F} = \sqrt{\frac{1 - p_F}{N p_F}}$$

of $\hat{p}_F$, is independent of the dimensionality of the random vector $\mathbf{X}$. However, for the estimation of small failure probabilities p_F, a very large number (proportional to $1/p_F$) of samples is needed for an accurate estimate. For this reason, advanced MCS techniques aim at reducing the variance of the estimator of p_F, with the effect that a smaller number of samples suffices. A well-established variance-reduction method, for example, is the *importance sampling* method (see, for example, [15]), in which the concentration of samples is shifted toward the failure domain [16]. However, just like many reliability methods, its performance deteriorates when the number of uncertain parameters increases. More recently, an efficient technique called *subset simulation* has been proposed by Au and Beck [5] in which the small failure probability p_F is expressed as a product of larger conditional failure probabilities, which can be estimated with fewer samples.

c. Line Sampling. The variance-reduction technique adopted in the present study is the mentioned line sampling method. This robust sampling technique has been successfully applied to problems involving high-dimensional reliability problems and is described in detail in [6]. Conceptually, in the line sampling procedure, conditional Monte Carlo simulation is applied. The key advantage compared with direct Monte Carlo simulation is that in the expression of the estimator [cf. Eq. (19)] the indicator function $1_F(\mathbf{X}^{(k)})$ is replaced by a quantity that, instead of stepping between 0 and 1, exhibits a lesser variation from one sample to the next. Consequently, the estimator's variability is greatly reduced and hence its accuracy for a given number of samples is larger.

Although the method has been discussed extensively elsewhere, its main features are presented in Appendix B to make the paper self-contained.

C. Role of Monte Carlo-Based Uncertainty Quantification in Verification and Validation Processes

As mentioned in the Introduction, uncertainty quantification is assigned an important role within the verification and validation (V&V) process of numerical solid mechanics models, as expressed in a recently released document of the ASME [3]. The aforementioned document subdivides the V&V activities in two branches (cf. Fig. 4 of the ASME guidelines), one departing from the mathematical model and the other from a physical model. Clearly, the methodologies described in the present paper are confined to the branch of the V&V process, which leads from the mathematical model through the computational model to the simulation outcomes. This branch is reproduced in Fig. 1.

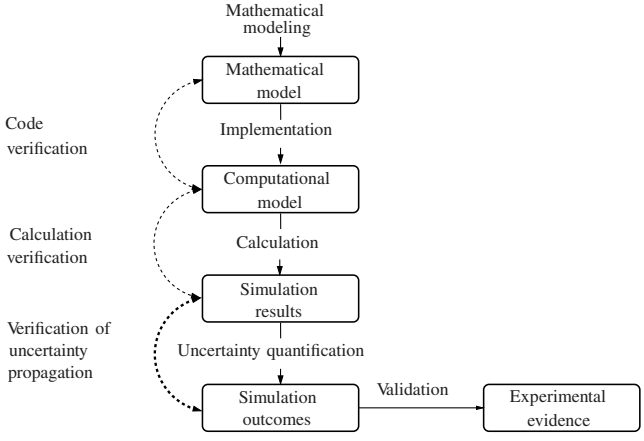

Fig. 1 Verification and validation activities associated with the mathematical model according to ASME.

With respect to their role in V&V, the Monte Carlo-based methodologies presented here may be classified into two categories. The first category includes the tools that lead to simulation results that can be used for the validation of the computational model; this category includes the Monte Carlo-based assessment of the modal scatter and of the frequency response. The second category encompasses the methods that are specifically geared toward assessing low failure probability of complex computational models of large-scale structures (i.e., for models of the entire system rather than of single components); this applies in particular to the line sampling method. Unless the required experimental data (e.g., large amounts of test data of the full-scale launcher-mounted satellite) can be produced with reasonable effort, these methods are not suitable for validation, but rather for prediction. In other words, these methods are meant to be used for predicting the reliability of the structure with the validated computational model.

In Sec. III.C.6, the preceding classification will be further discussed and applied to the analysis steps carried out in the present case study.

Finally, one aspect of V&V is mentioned here: namely, that of verification of the uncertainty quantification step. This aspect is not addressed in the ASME guidelines on V&V, but it is explicitly included in the bottom left portion of Fig. 1; the verification of the uncertainty propagation makes sure that the uncertainties in the quantities of interest are predicted correctly by the adopted uncertainty quantification algorithm. The methodology based on Monte Carlo simulation includes the tools needed to perform the verification, because along with the probabilistic statements on the quantities of interest, the error associated with these statements can be quantified, for instance, in terms of confidence intervals.

III. Satellite Structure: Uncertainty and Reliability Analysis

A. Introductory Remarks

The development of the uncertainty analysis tools described in the previous section was driven by the need to process uncertainties in large FE systems. In this section, the application of these tools to a set of analysis problems arising in the context of spacecraft dimensioning and verification is described. More specifically, the response of a satellite-launcher system is analyzed.

B. Probabilistic Modeling Assumptions

As mentioned in Sec. II.B.4, for complex FE models, it is very hard to identify a priori the uncertain parameters with great impact on the response quantities of interest and those with negligible impact. Furthermore, various response quantities (stresses, interface forces, and accelerations) at various locations of the structure are relevant, with different sensitivities. In addition, limited specific information on the degree of uncertainty associated with the various parameters is available.

To ensure as great a generality as possible, a conservative approach has been taken and as many FE model parameters as possible have been treated as random variables. This way, the risk of ignoring the uncertainties in parameters with a great impact on the response is minimized.

This generality, however, comes at a price and leads to an unusually large number of random variables: approximately 1300 for both the satellite (Sec. III.C) and the launcher (Sec. III.D). The levels of variability are selected on the basis of data available in the literature [1,2,17,18]. Details on the assumed degree of variability are included in Appendix A. For instance, for Young's moduli of isotropic materials, the COV σ/μ was assumed to be 8%. The assumed COV range was from 4 to 12%.

The mean values were set equal to the nominal values of the deterministic FE model. The probability distribution of the random properties is assumed to be Gaussian, with the exception of the damping. This assumption is sufficiently accurate, given the lack of hard data. Because of the small COV, the probability of occurrence of negative values for properties such as Young's modulus is practically

zero. This does not apply to the damping, however, which is usually affected by greater uncertainty. In this case, a log-normal distribution with a COV of 20% for modal damping and of 25% for structural damping has been assumed.

It should be noted that the spatial correlation of the uncertain parameters has been neglected in this study, for two reasons, as described in the following. First, one of the objectives of this study was to show that a large-scale uncertainty analysis can be performed without much additional effort using an existing (deterministic) finite element model. Because the FE models used for industrial applications in most cases exhibit constant model properties for each individual component, these properties are typically parametrized with a single quantity for each component. This is, of course, not suitable for a stochastic finite element model, because the spatial fluctuations of properties require a separate parameter for each element. To satisfy this requirement, the analyst would have to substantially modify the existing deterministic model. The second reason for not modeling the spatial correlation of the uncertain parameters in this study is that statistical information on the correlation distance of properties is extremely scarce.

Once the uncertain FE model parameters have been defined according to Table 1, the uncertainty analysis software code FE_RV [19] has been used to perform the analyses as described in this section. With respect to Table 1, it should also be noted that it has been assumed that no correlation exists between the various uncertain properties, because no statistical information suggesting otherwise is available. Clearly, in the presence of solid information on existing correlations, this could easily be accounted for, as the adopted software code FE_RV is capable of injecting arbitrary correlations.

C. Satellite Structural Analysis

1. *Description of the Deterministic Numerical Model*

The numerical model of the satellite is a refined finite element model for the commercial FE software code MSC.Nastran, with roughly 120,000 DOF, provided by ESA. The FE model is shown in Fig. 2; detailed information concerning the model can be found in [20–22].

Table 1 Assumed COV of uncertain finite element model parameters

Property	COV σ/μ
Isotropic material	
Young's modulus	8%
Poisson's ratio	3%
Shear modulus	12%
Mass density	4%
Orthotropic shell element material	
Young's modulus	8%
Shear modulus	12%
Mass density	4%
Solid element anisotropic material	
Material property matrix	12%
Mass density	4%
Simple beam	
Section dimension	5%
Nonstructural mass	8%
Layered composite material	
Nonstructural mass	8%
Thickness of plies	12%
Orientation angle	$\sigma = 1.5$
Shell element	
Membrane thickness	4%
Nonstructural mass	8%
Spring element	
Stiffness	10%
Concentrated mass	
Mass	3%
Damping	
Modal damping	20%
Structural damping	25%

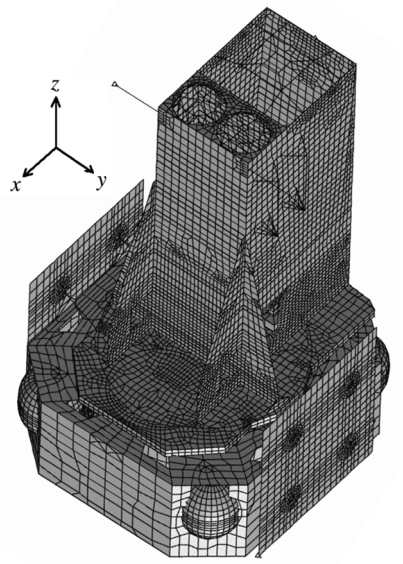

Fig. 2 INTEGRAL satellite (model provided by ESA/ESTEC).

2. *Modal Scatter*

The first step in the analysis of the satellite consists of the normal modes analysis, according to Eq. (2). Relying on the formulation described in Sec. II.B.3, the uncertainty in the eigenfrequencies of the satellite (due to the uncertainties in the FE model parameters, as described in the previous section) has been analyzed. Figure 3 shows the approximate probability density functions (PDFs) of the eigenfrequencies. Eigenfrequencies 1–4 (shown in Fig. 3a) are well separated and Gaussian. However, starting from mode 5 (shown in Fig. 3b), a significant overlap between the PDFs of various modes can be observed. In these cases (due to the high modal density around 37 Hz), the weighting procedure represented by Eqs. (11–13) is instrumental in propagating the uncertainties in a meaningful way. Postprocessing the ensemble of eigenfrequencies indiscriminately according to their sequential number would result in grossly misleading PDFs and COV.

3. *Frequency Response Scatter*

In addition to the eigenfrequencies, the uncertainty in the frequency response of the satellite has been analyzed for the frequency range of 5–100 Hz. The loading is deterministic and consists of a harmonic acceleration in the x direction. The prescribed acceleration amplitude is $1\ g$ for $f < 25$ Hz and $0.8\ g$ for $f > 25$ Hz.

An ensemble of 1500 MCS samples of the frequency response functions has been produced, with the uncertain parameters sampled according to the probabilistic modeling assumptions reported in Table 1.

In Figs. 4–6, the fractiles of the frequency response in the range of 30–100 Hz are depicted. For a given frequency, the value of each fractile shown in the figures indicates the level of the frequency response that is not exceeded by the corresponding percentage of the samples. For instance, the value of the 99.8% fractile at the frequency of 60 Hz in Fig. 4 is approximately 5×10^7 N/m^2, meaning that only 0.2% of the samples will exceed that value for an excitation of 60 Hz.

Figures 4–6 refer to three different degrees of uncertainty in the damping. More specifically, the COV of the damping is 0% in Fig. 4 (i.e., no uncertainty in the damping), 20% in Fig. 5, and 40% in Fig. 6. It should be noted that the uncertainty in the damping is in addition to that in the other FE model parameters, as listed in Table 1. For the nominal damping ratios $\{\zeta_j\}_{j=1}^m$, 1.5% of critical damping was assumed for frequencies below 30 Hz and 2.5% above 30 Hz.

The response quantity (to which the results shown here refer) is the maximum von Mises stress in the beam connecting the solar panel with the satellite structure. Generally speaking, the variability of the

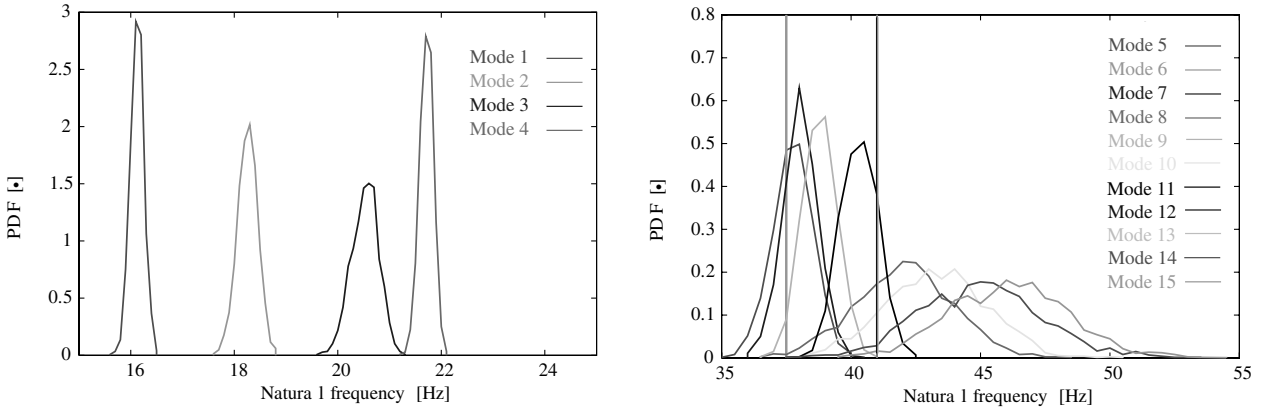

Fig. 3 Approximate PDFs of the natural frequencies for the eigenmodes 1–15 of the INTEGRAL satellite, upon resolution of the eigenfrequency-eigenmode correspondence.

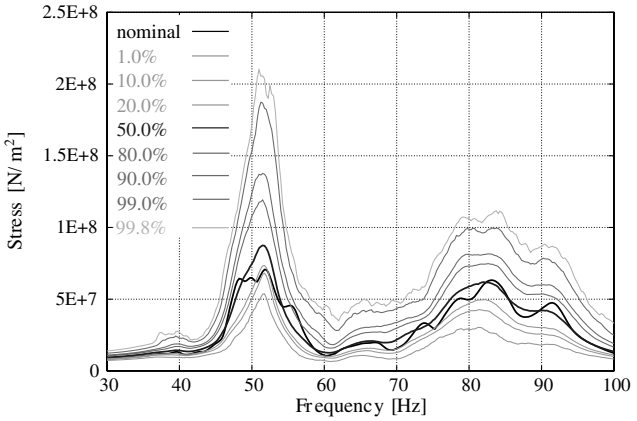

Fig. 4 Maximum von Mises stress in the solar-panel connecting beam of satellite due to harmonic support excitation (frequency response analysis); no uncertainty in the damping.

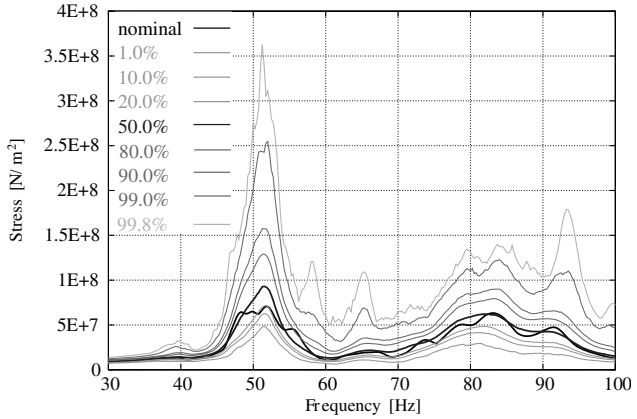

Fig. 5 Maximum von Mises stress in the solar-panel connecting beam of satellite due to harmonic support excitation (frequency response analysis); uncertainty in the damping is 20% COV

response is rather high, even for deterministic damping, as shown in Fig. 4. However, as Figs. 5 and 6 show, introducing the uncertainty in the damping leads to considerable additional scatter in the frequency response, with the effect of doubling some of the peak values of the fractiles in the case of a 40% COV. In particular, it should be noted how the extreme amplitudes (represented, for example, by the 99.8-percentile curve), drastically increase at the resonance frequency around 50 Hz (the different scale on the ordinate of Figs. 4–6 should be noted).

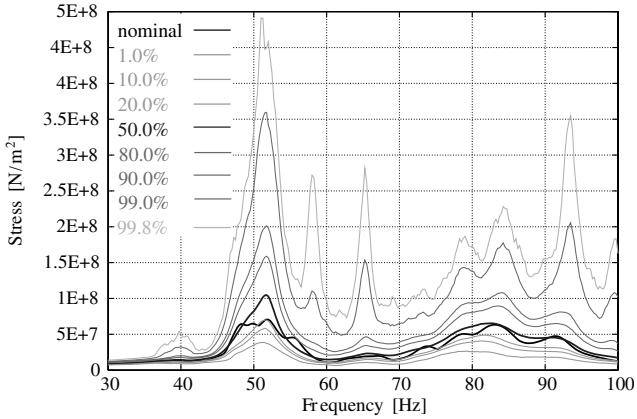

Fig. 6 Maximum von Mises stress in the solar-panel connecting beam of satellite due to harmonic support excitation (frequency response analysis); uncertainty in the damping is 40% COV

4. Sensitivity Analysis

In addition to the dynamic load cases, the satellite has been also analyzed under a static load case. Specifically, gravity-type loading with a magnitude of 6 g in the negative z direction and 1 g in the x direction (see Fig. 2) has been applied. The quantity of interest in this case is the shear force in one of the solar-panel hold-down beams.

The estimation of the gradient of the shear force has been performed by using the algorithm outlined in Sec. II.B.4. In total, just 229 response evaluations were needed to estimate the gradient with an accuracy of 98.86%. Hence, with less than 20% of the samples needed by a finite difference computation, the gradient could be estimated with excellent accuracy.

Table 2 lists those parameters of the FE model of the International Gamma Ray Astrophysics Laboratory (INTEGRAL) satellite that emerged as the most influential parameters from the gradient estimation.

The algorithm hence confirms the intuitive result that the most important parameter (relative weight 83.1%) is the nonstructural mass of the solar panel held by the beam under consideration. Figure 7 highlights the solar panels, the nonstructural mass of which is the parameter with the greatest impact on the shear force in the considered solar-panel hold-down beam.

5. Reliability Analysis

a. Static Load Case. For the static load case introduced in Sec. III.C.4, a reliability analysis has been performed with respect to the shear force in the solar-panel hold-down beam [23]. For this purpose, the line sampling method outlined in Sec. II.B.5 has been employed. The important direction used in the sampling scheme

Table 2 Summary of the parameters of the FE model with the greatest impact on the shear force in the solar-panel hold-down beam (static load case)

Rank	Relative importance	Parameter description	Element type
1	83.1%	Nonstructural mass solar panel (solar panel)	Shell
2	39.6%	Width of solar-panel hold-down beams	Beam
3	23.7%	Young's modulus solar-panel hold-down beams	Beam
4	19.7%	Height of solar-panel hold-down beams	Beam
5	16.3%	Composite-ply thickness	Shell
6	14.8%	Height diagonal stiffener	Beam
7	9.1%	Young's modulus diagonal stiffener	Beam
8	1.3%	Orientation-angle composite ply	Shell

consisted of the gradient at the nominal point, as described in the previous section on sensitivity analysis. Figure 8 shows the excellent performance of the line sampling method for this load case. Each bar corresponds to a particular level of the limit state, represented in this case by the critical sliding force F_{sliding} at the solar-panel connector beam. The plot indicates, for instance, that if the failure threshold value of F_{sliding} is 1150 N, then the probability of failure is 1 in 10 million (10^{-7}). In addition, each bar is marked with the corresponding error bars, which indicate the $\hat{p}_F \pm \sigma_{\hat{p}_F}$ interval, where $\sigma_{\hat{p}_F}$ is the standard deviation of the estimated value of the failure probability. It is apparent that the intervals (and hence the error) are very narrow, even for very low failure probabilities.

To verify the predictions of the failure probabilities obtained via line sampling, the results have been compared with direct Monte Carlo simulation (for $p_F \geq 10^{-2}$) and with subset simulation [5] (for p_F as low as 10^{-6}). Figure 9 shows that the line sampling results match direct MCS (≈400 simulations) perfectly. Furthermore, the line sampling results are in good agreement with the results of subset simulation. Two sets of subset simulation have been carried out, both with the conditional p_F set to 10% and with a rejection rate of 35%. As the two sets have been produced using a different seed for the

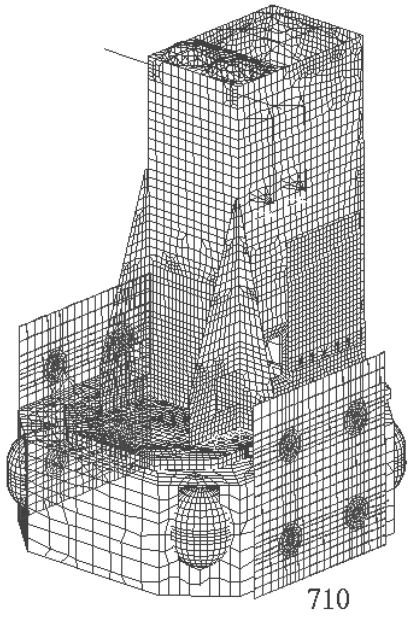

Fig. 7 Gradient visualization; rank 1 of most influential parameters; nonstructural mass of solar panels.

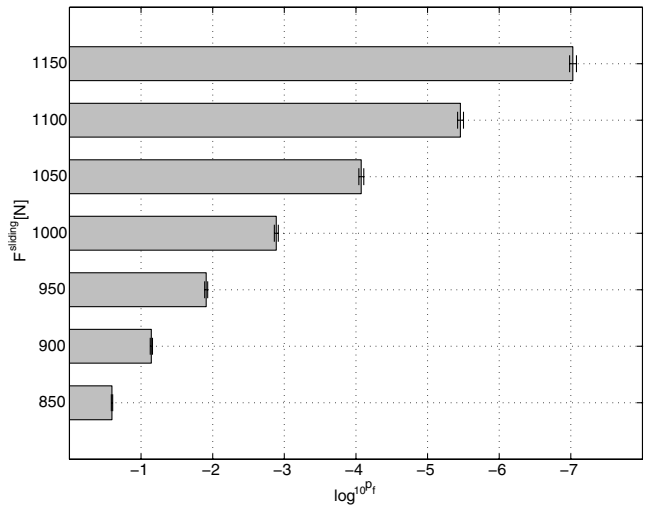

Fig. 8 Exceedance (failure) probability vs critical sliding force at solar-panel connector beam (F_{sliding}).

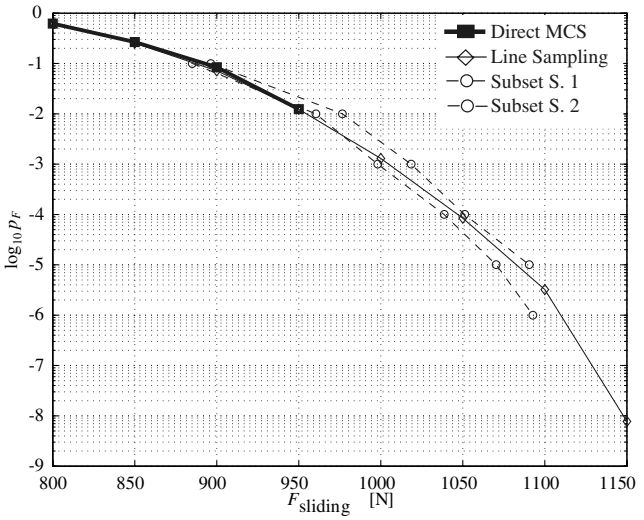

Fig. 9 Verification of failure probabilities computed with line sampling, by comparison with direct MCS and subset simulation; static load case.

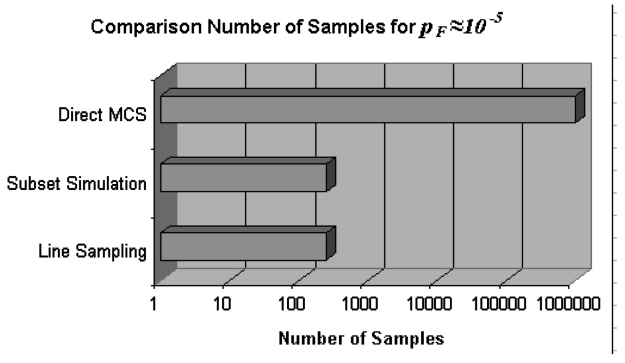

Fig. 10 Comparison of number of samples required for line sampling, subset simulation and direct MCS; number of samples on log scale.

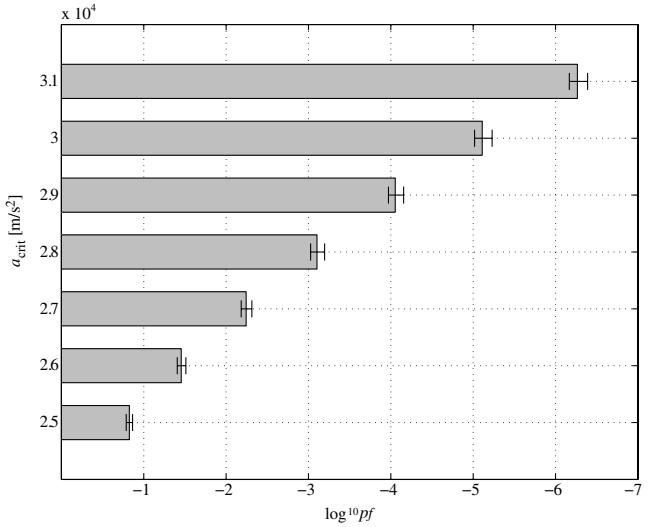

Fig. 11 Exceedance (failure) probability vs critical average acceleration in the range of 10–30 Hz.

random number generator, the predicted p_F differ from each other. The associated savings in CPU time become apparent from Fig. 10; whereas direct MCS requires 1 million samples to estimate a p_F of 10^{-5}, only around 250 samples are necessary for both line sampling and subset simulation.

b. Dynamic Load Case. The reliability analysis has also been performed for the dynamic load case introduced in Sec. III.C.3. The response quantity of interest in this case consists of the average acceleration at the extremity of one of the sun acquisition sensor booms over the frequency band 10–30 Hz. Figure 11 shows the line sampling results for the dynamic load case. The performance of the method is again very convincing, because a relatively low number of samples already enables an accurate estimation of low failure probabilities. This is indicated by the narrow intervals that delimit the range $\hat{p}_F \pm \sigma_{\hat{p}_F}$. Verification results for the failure probability estimates are shown in Fig. 12. Again, excellent agreement with direct MCS results (2800 samples) can be observed.

6. Verification and Validation Aspects of the Satellite Uncertainty and Reliability Analysis

a. Verification. The aspects of code and calculation verification [3] are not within the focus of the present case study, notwithstanding that corresponding activities (e.g., mesh refinement based on convergence analysis) have been performed. However, the

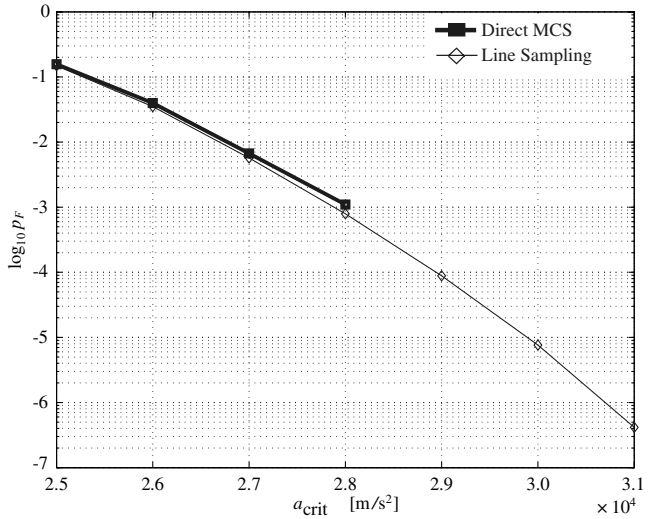

Fig. 12 Verification of failure probabilities computed with line sampling by comparison with direct MCS; dynamic load case; 10–30 Hz.

methods presented and applied here do play an essential role with respect to a verification aspect that has been omitted in the ASME guidelines: namely, the verification of the uncertainty quantification. In the present case study, this type of verification consists of controlling the error introduced by the finite sample size in Monte Carlo-based uncertainty quantification methods. In Fig. 1, this type of verification is denoted as verification of uncertainty propagation. The methodologies advocated in this paper meet the needs introduced by this additional verification step, in that they provide an estimate of the error in form of confidence intervals or the standard error (i.e., the standard deviation of the estimator). The latter error estimate is indicated in Figs. 8 and 11 in the form of error bars superimposed with the estimates.

b. Validation with Respect to the Deterministic Model. In the present case study, the considered satellite is a one-of-a-kind structure; the full-scale experimental modal analysis has been performed and used to validate the model. A deterministic numerical model was used in the validation process. According to the ASME (cf. Figure 4 in the ASME guidelines), however, the experimental outcome should be used to validate the computational model only after the uncertainty associated with the latter has been quantified.

c. Modal Analysis Within the Validation Process. The result of the uncertainty quantification of the modal analysis as described in Sec. III.C.2 (see Fig. 3) can be considered as simulation outcomes to be used for the validation of the computational model. The results of the quantification of the modal scatter are therefore instrumental for the validation.

d. Frequency Response Functions. As opposed to the modal scatter, the simulation outcomes of the frequency response scatter analysis (Sec. III.C.3) have a purely predictive character (see Figs. 4–6). Indeed, the fractiles derived from these outcomes relate to probability levels that would be out of reach for direct validation based on experiments with a similar amount of samples of the system. Hence, these results are based on a numerical model that is assumed to be validated.

e. Sensitivity Analysis. According to the ASME guidelines, sensitivity analysis plays an important role during the development of the conceptual model, as it helps the modeler to identify the physical phenomena that are relevant for quantities of interest. In the present case, the sensitivity analysis (described in Sec. III.C.4) essentially serves two purposes: First, the relative impact of the uncertainties on the quantity of interest is quantified. This delivers valuable information for the validation of the model; indeed, the modeler may focus his efforts with respect to model revision and updating on parameters with a high relative impact. Second, the ensemble of relative importance measures of all parameters is a critical ingredient for the reliability estimation algorithm (line sampling here). In this case, the sensitivity analysis transcends its role within the validation process and is instead used for predictive purposes; this will also be discussed in the next paragraph.

f. Reliability Analysis. As already remarked in Sec. II.C, the advanced simulation method for reliability analysis (namely, line sampling) has been specifically developed for the assessment of low failure probabilities of complex computational models of large-scale structures. Hence, it is suitable for prediction, but not for validation, because the required experimental data cannot be obtained.

D. Load-Coupled Dynamic Analysis (Launcher and Satellite)

Analyses of the coupled system launcher payload are performed extensively in the aerospace field to derive loading specifications for payload (e.g., satellite) design and verification. A Monte Carlo simulation-based uncertainty analysis has been performed by the authors [24] in which the launcher payload assemblage of the Ariane-5 launcher and the INTEGRAL satellite were analyzed. In that case, 1500 Monte Carlo samples have been produced for two different load cases (one transient load case and one frequency response analysis) under consideration of uncertainties in the launcher model, the satellite model, and the loading.

The results showed a very significant impact of the uncertainties in the parameters of the FE models on the quantities of interest. In

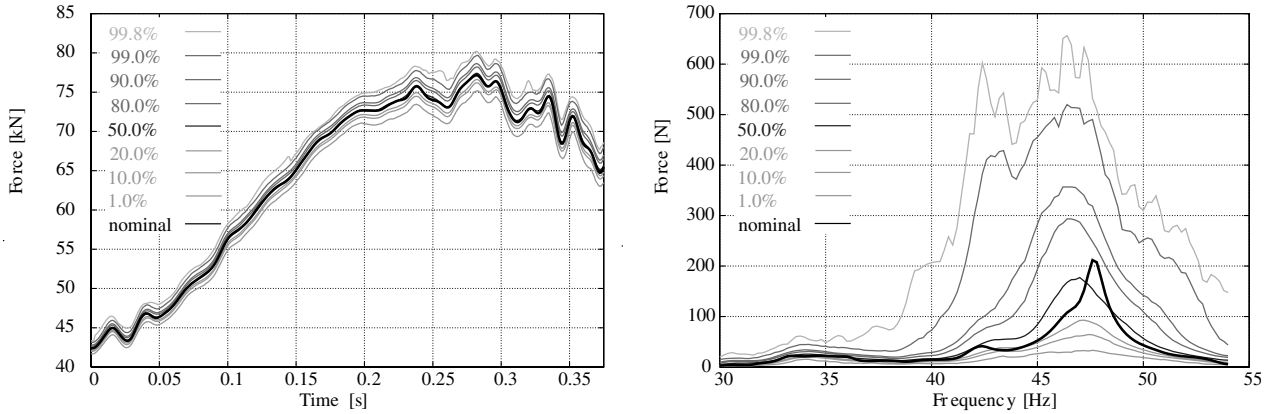

a) b)

Fig. 13 Fractiles of interface force between launcher and satellite due to launcher scatter; end-of-booster pressure oscillation load case (left) and liftoff load case (right) (cf. [24]).

particular, the uncertainties in the launcher lead to enormous scatter in the frequency response of the so-called end-of-booster pressure oscillation load case of the Ariane-5 launcher. This is documented in Fig. 13b, in which each line corresponds to one percentile of the frequency response. Clearly, the percentiles are quite far apart from each other, thus indicating a very pronounced random scatter of the response. In comparison, in the transient liftoff load case (Fig. 13a), the scatter induced by the uncertainty in the launcher properties is moderate. For a detailed treatment of the stochastic coupled-load analysis, the reader is referred to [24].

1. Verification and Validation Aspects of the Load-Coupled Dynamic Analysis

With reference to the terminology of the ASME guidelines for verification and validation, the satellite model in Sec. III.C corresponds to the system model, whereas in the present case, the so-called reality of interest is constituted by the launcher-satellite assembly (i.e., the satellite plays the role of a subassembly). Given that no experimental evidence is available for the launcher-satellite system, the associated results of the uncertainty quantification fulfill an exclusively predictive character.

IV. Conclusions

In this paper, a novel framework for the uncertainty and reliability analysis of large numerical models of complex aerospace applications is proposed. The key advantage of the procedure is that it is robust with respect to the number of uncertain parameters and hence remains applicable to large FE systems with many sources of uncertainty. Consequently, the method remains feasible even in combination with refined state-of-the-art deterministic FE models.

The two newly developed cornerstones of the procedure are a highly efficient algorithm for the estimation of the relative importance of parameters, which filters out those parameters with the greatest impact on a given response quantity. This algorithm plays a pivotal role in combination with variance-reduction Monte Carlo procedures: in this case, the so-called line sampling scheme for the estimation of low failure probabilities in problems with a large number of uncertain parameters. This gives the procedure a competitive edge over alternative approaches, because direct MCS is infeasible in this case and numerous alternative methods lose performance when the number of uncertain parameters increases.

The application of the proposed procedure to the static and dynamic reliability analysis of the satellite shows that these tools make it possible to estimate low failure probabilities of systems with large numbers of uncertain parameters at reasonable computational costs.

The array of analysis tasks addressed in this paper includes the modal and frequency response analysis of a satellite structure, as well as coupled-load analyses, taking into account uncertainties in the satellite, the launcher, and the loading. For both the frequency response analysis of the satellite alone and the coupled-load analyses of the launcher-satellite assembly, the results show that the uncertainty in the mechanical model parameters has very strong effects on the predicted responses and should be of concern for the analysts and designers of these structures.

The availability of the method, as described here, will direct the goal-oriented collection of data on the properties of large-scale structures. Furthermore, the methodology integrates well with the verification and validation processes recently introduced by the ASME in the form of guidelines that explicitly call for uncertainty quantification of computational models before their validation.

Appendix A: Gradient Estimation Algorithm

The essential steps of the algorithm are as follows. The response is computed at the nominal value of the input parameters:

$$r^{(0)} = r(\mathbf{x}^{(0)})$$

Next, an initial set of N_0 samples is generated with direct Monte Carlo sampling, however, using a reduced standard deviation for the input parameters. With reference to Eq. (6), this means that if the standard deviations corresponding to the CDFs of the uncertain parameters are denoted by $\{\sigma_{x_j}\}_{j=1}^{d}$, instead of using the set of random variables $\mathbf{X}$ defined in Eq. (5), the initial set of Monte Carlo samples is generated using a modified set of random variables $\hat{\mathbf{X}} = [\hat{X}_1\ \hat{X}_2\ \cdots\ \hat{X}_d]$, for which the standard deviations are denoted as $\{\sigma_{\hat{x}_j}\}_{j=1}^{d}$, where $\sigma_{\hat{x}_j} = \sigma_{x_j}/C$. A suitable value for the reduction factor is $C = 10$. The use of random input parameter samples with a reduced standard deviation helps to ensure that the response remains within the quasi-linear range with respect to the input parameters.

For each sample k of the N_0 samples, the response $r(\mathbf{x}^{(k)})$ and the corresponding deviation from the nominal response $\bar{r}$ are evaluated [i.e., $b^{(k)} = r(\mathbf{x}^{(k)}) - \bar{r}$].

With the available set of samples, the sample correlation between each input parameter and the response is evaluated. A ranking of the relative importance of all uncertain input parameters $\{x_j\}_{j=1}^{d}$ is then established, based on the absolute value of the sample correlation.

For the L most important variables, the corresponding partial derivative is determined with by finite differences [i.e., using Eq. (16)]. The integer value L is user-defined; for the sake of efficiency $L \ll d$, as a rule of thumb, $L = 10$ is suggested.

The actual relative importance is assessed with Eq. (15) and compared with the average contribution of each parameter to the total standard deviation of the response, $\bar{s} = \sigma_{\hat{r}}/\sqrt{N_0}$. If it is below that value, then the so-called failure counter variable is incremented. Indeed, the fact that a parameter that was estimated to be of major importance turns out to account for less than the average contribution

of each parameter to the total standard deviation is considered as a failure in the economy of the algorithm.

Whenever the failure counter exceeds a certain user-defined threshold value (e.g., 10), an additional set of MCS samples is generated and the algorithm proceeds from there.

The influence of those parameters for which the partial derivatives have been computed based on the importance ranking is removed from the ensemble of response deviations: $\{b^{(k)}\}_{k=1}^{N_0}$. The ensemble of the variations that have been modified in the described way is denoted as $\{c_U^{(k)}\}_{k=1}^{N_0}$.

Next, the exit criterion is probed. If the achieved accuracy exceeds the user-defined accuracy threshold, that is, if

$$\epsilon = \sqrt{1 - \frac{\|\boldsymbol{c}_U\|}{\|\boldsymbol{b}\|}} \geq \epsilon_{\min}$$

then convergence has been reached. A typical value for the threshold is $\epsilon_{\min} = 0.95$. It should be noted that convergence is guaranteed after evaluating, at most, d (i.e., *all*) partial derivatives. If the accuracy of the gradient estimate is not sufficient, the relative importance of additional parameters has to be evaluated.

Appendix B: Line Sampling

The line sampling procedure is an advanced simulation method for the efficient estimation of the probability of rare events such as the failure of a structural component. Conceptually, conditional Monte Carlo simulation is applied. Figure B1 synthesizes the essence of the method in the context of a two-dimensional problem [i.e., $d = \dim(\mathbf{X}) = 2$].

The key feature of the method consists of the evaluation of samples along a set of lines, for which one exemplary line $l^{(j)}$ is denoted by $l^{(j)}(c, \mathbf{e}_{\boldsymbol{\alpha}})$ in Fig. B1. The points in the input parameter space at which samples are taken are indicated by the small circles located on line $l^{(j)}$. The goal behind the evaluation of the response and hence of the performance function $g(\mathbf{X})$ for these samples is the identification of the point of intersection between line $l^{(j)}$ and the limit-state surface $g(\mathbf{X}) = 0$, which separates the safe domain from the failure domain (shaded area). The length of the line segment between line $\mathbf{X}^{\perp}$ and the point of intersection is denoted by $\bar{c}^{(j)}$. Repeating this operation for a sufficient number N of samples and obtaining the corresponding set of distances $\{\bar{c}^{(j)}\}_{j=1}^{N}$ leads to an estimate $\bar{p}_F$ of the probability of failure:

$$\bar{p}_F = \frac{1}{N}\sum_{j=1}^{N} p_F^{(j)} \tag{B1}$$

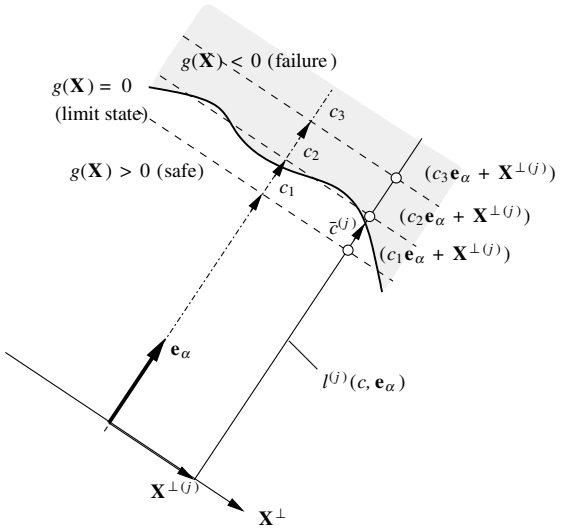

Fig. B1 Schematic sketch for line sampling procedure.

where $p_F^{(j)} = \Phi(-\bar{c}^{(j)})$. In the preceding equation, Φ denotes the Gaussian cumulative distribution function. In addition to the estimate itself, an estimate of the associated variance $\sigma_{\bar{p}_F}^2$ can be obtained as well, which provides a means for controlling the accuracy of the estimate and an exit criterion for the algorithmic implementation:

$$\sigma_{\bar{p}_F}^2 = \frac{1}{N-1}\sum_{j=1}^{N}\left(p_F^{(j)} - \bar{p}_F\right)^2 \tag{B2}$$

As mentioned in Sec. II.B.5, the key advantage over direct Monte Carlo simulation is that in Eq. (B1), the indicator function $1_F(\mathbf{X}^{(k)})$ of Eq. (19) is replaced with $p_F^{(j)}$, which exhibits less variation from one sample to the next. This is a direct consequence of the situation depicted in Fig. B1, in which the intersection with the limit-state surface is at approximately the same distance from $\mathbf{X}^{\perp}$ for each of the lines, and hence, according to Eq. (B1), the corresponding values of $p_F^{(j)}$ are close. The line sampling method has a superior efficiency (compared with direct Monte Carlo simulation) because it makes use of information on the limit-state function and takes samples accordingly, as shown in Fig. B1. In contrast, in direct Monte Carlo simulation, the algorithm takes samples in a completely random (and hence blind) fashion, and the membership to the safe or the failure domain (shaded area in Fig. B1) is verified implicitly for each sample.

The direction of the lines along which the samples are taken is called the *important direction*. In fact, the most difficult step of the procedure typically consists of the identification of this important direction in the input parameter space, represented by the unit vector $\mathbf{e}_{\boldsymbol{\alpha}}$. A suitable direction is provided in many cases by the gradient (or its approximation) evaluated at the nominal point in the input parameter space. Although the exact computation of the gradient can be very CPU-intensive for large numbers d of uncertain input parameters, an accurate approximation can be obtained using the novel algorithm described in Sec. II.B.4. On the other hand, in the presence of a priori information (e.g., on the basis of experience and physical reasoning), a valid important direction might be assumed without the need of extensive prior analysis. Finally, it should be noted that the method is robust and that its properties have been shown to converge to those of direct MCS in the worst-case scenario, whereas in the great majority of cases, a significant reduction of the variance (and hence of the required number of samples) can be achieved. That property of this novel procedure is essential for the feasibility of structural reliability analysis of large-scale structural models.

Acknowledgments

This research was partially supported through the ESA/European Space Research and Technology Centre (ESTEC) General Support Technology Programme contract 16144/02NL/PA and through the Fonds zur Förderung der Wissenschaftlichen Forschung (Austrian Research Council) contract P19781-N13, which is gratefully acknowledged by the authors. Special thanks are due to Michel Klein, Head of the Structures Section of ESA/ESTEC, for his most valuable advice and continuous support. The supply of the finite element model by ESA/ESTEC is also deeply appreciated.

References

[1] Esnault, P., and Klein, M., "Factors of Safety and Reliability—Present Guidelines & Future Aspects," *Proceedings of the Conference on Spacecraft Structures, Materials & Mechanical Testing*, SP-386, ESA, Noordwijk, The Netherlands, 27–29 Mar. 1996, pp. 109–119.

[2] Klein, M., Schuëller, G., Deymarie, P., Macke, M., Courrian, P., and Capitanio, R. S., "Probabilistic Approach to Structural Factors of Safety in Aerospace," *Proceedings of the International Conference on Spacecraft Structures and Mechanical Testing*, Cépadués-Editions, Paris, 1994, pp. 679–693.

[3] "Guide for Verification and Validation in Computational Solid Mechanics," American Society of Mechanical Engineers, Rept. V&V 10-2006, New York, 2006.

[4] Ripley, B., *Stochastic Simulation*, Wiley, New York, 1987.
[5] Au, S.-K., and Beck, J., "Estimation of Small Failure Probabilities in High Dimensions by Subset Simulation," *Probabilistic Engineering Mechanics*, Vol. 16, No. 4, 2001, pp. 263–277. doi:10.1016/S0266-8920(01)00019-4
[6] Schuëller, G. I., Pradlwarter, H. J., and Koutsourelakis, P., "A Critical Appraisal of Reliability Estimation Procedures for High Dimensions," *Probabilistic Engineering Mechanics*, Vol. 19, No. 4, 2004, pp. 463–474. doi:10.1016/j.probengmech.2004.05.004
[7] Pradlwarter, H. J., "Relative Importance of Uncertain Structural Parameters, part I: Algorithm," *Computational Mechanics*, Vol. 40, No. 4, 2007, pp. 627–635. doi:10.1007/s00466-006-0127-9
[8] Pellissetti, M. F., Pradlwarter, H. J., and Schuëller, G. I., "Relative Importance of Uncertain Structural Parameters, Part 2: Applications," *Computational Mechanics*, Vol. 40, No. 4, 2007, pp. 637–649. doi:10.1007/s00466-006-0128-8
[9] Craig, R., *Structural Dynamics—An Introduction to Computer Methods*, Wiley, New York, 1981.
[10] Fransen, S., "Data Recovery Methodologies for Reduced Dynamic Substructure Models with Internal Loads," *AIAA Journal*, Vol. 42, No. 10, 2004, pp. 2130–2142. doi:10.2514/1.6187
[11] Papadrakakis, M., and Papadopoulos, V., "Robust and Efficient Methods for Stochastic Finite Element Analysis Using Monte Carlo Simulation," *Computer Methods in Applied Mechanics and Engineering*, Vol. 134, Nos. 3–4, 1996, pp. 325–340. doi:10.1016/0045-7825(95)00978-7
[12] Papoulis, A., *Probability & Statistics*, Prentice–Hall, Englewood Cliffs, NJ, 1990.
[13] Ewins, D. J., *Modal Testing: Theory, Practice, and Application*, 2nd ed., Research Studies Press, Baldock, England, U.K., 2000.
[14] Friswell, M., and Mottershead, J., *Finite Element Model Updating in Structural Dynamics*, Kluwer Academic, New York, 1995.
[15] Rubinstein, R., and Kroese, D., *Simulation and the Monte Carlo Method*, Wiley, New York, 2007.
[16] Schuëller, G. I., and Stix, R., "A Critical Appraisal of Methods to Determine Failure Probabilities," *Structural Safety*, Vol. 4, No. 4, 1987, pp. 293–309. doi:10.1016/0167-4730(87)90004-X
[17] Székely, G. S., Teichert, W. H., Brenner, C. E., Pradlwarter, H. J., Klein, M., and Schuëller, G. I., "Practical Procedures For Reliability Estimation of Spacecraft Structures And Their Components," *AIAA Journal*, Vol. 36, No. 8, 1998, pp. 1509–1515. doi:10.2514/2.545
[18] Simonian, S., "Survey of Spacecraft Damping Measurements: Applications to Electro-Optic Jitter Problems," *The Role of Damping in Vibration and Noise Control*, Vol. 5, American Society of Mechanical Engineers, New York, Sept. 1987, pp. 287–292.
[19] FE_RV, Software Package, Ver. 1.0, Inst. für Mechanik, Univ. of Innsbruck, Innsbruck, Austria, 1999.
[20] Notarnicola, M., Paron, A., Tizzani, L., and Evans, E., "INTEGRAL–Structural Mathematical Model Description and Dynamic Analysis Results," Alenia Aerospazio Space Div., TR INT-TN-Al-0089, Turin, Italy, 15 Apr. 1998.
[21] Moreno, C., "INTEGRAL—Service Module Structure Mathematical Model Description," CASA Space Div., TR INT-TN-CAS-1002, 1st ed., Madrid, Spain, Apr. 1998.
[22] Oxfort, M., "INTEGRAL—PLM Payload Module Structure FEM Description," Oerlikon-Contraves BU Space, TR INT-RP-OCW-0002, 2nd ed., Zürich-Seebach, Switzerland, Dec. 1997.
[23] Pellissetti, M. F., Schuëller, G. I., Pradlwarter, H. J., Calvi, A., Fransen, S., and Klein, M., "Reliability Analysis of Spacecraft Structures Under Static and Dynamic Loading," *Computers and Structures*, Vol. 84, No. 21, 2006, pp. 1313–1325. doi:10.1016/j.compstruc.2006.03.009
[24] Pellissetti, M. F., Fransen, S., Pradlwarter, H. J., Calvi, A., Kreis, A., Schuëller, G. I., and Klein, M., "Stochastic Launcher-Satellite Coupled Dynamic Analysis," *Journal of Spacecraft and Rockets*, Vol. 43, No. 6, 2006, pp. 1308–1318. doi:10.2514/1.21154

G. Agnes
Associate Editor